

DESIGN AND VALIDATION OF A FOREHEAD PULSE OXIMETER FOR MILITARY MEDICAL EVACUATION

Dominik Sondej¹), Paweł Oskwarek²), Rafał Sokółowski²), Michał Rząd²), Adam Machowicz²), Tadeusz Sondej¹), Paweł Dąbal¹), Piotr Łubkowski¹)

1) Military University of Technology, Faculty of Electronics, Gen. S. Kaliskiego 2, 00-908 Warsaw, Poland (✉ dominik.sondej@wat.edu.pl)

2) Military Institute of Medicine, ul. Szaserów 128, 04-141 Warsaw, Poland

Abstract

This article presents the design, implementation, and validation of an SpO₂ sensor prototype, developed as part of a military medical evacuation system. A reflectance method was chosen for SpO₂ measurement, allowing for readings to be taken from any location on the body, unlike the traditional transmissive method. The sensor is designed as a headband worn on the forehead, a well-perfused area, ensuring that the placement does not hinder soldier mobility. The sensor construction utilized the optical module SFH7072, the AFE4410 integrated circuit, and an STM32L5 microcontroller. To obtain accurate SpO₂ readings, signal processing techniques, including filtering, were applied, along with the development of algorithms to calculate SpO₂ from photoplethysmographic (PPG) signals. The prototype underwent validation tests using a comprehensive experimental setup. The prototype achieved an A_{RMS} (root mean square difference) value of 3.0%, meeting the ISO 80601-2-61 standard for reflectance sensors, which recommends an A_{RMS} ≤ 3.5%.

Keywords: photoplethysmography, PPG, SpO₂, oxygen saturation, wearable forehead pulse oximeter, SpO₂ validation study.

1. Introduction

Modern armed forces face the challenge of not only investing in the development of advanced weapons, protective gear, drones, and vehicles, but also in systems capable of remotely monitoring the health status of soldiers in combat situations. Medical evacuation during combat missions is crucial to safely transporting injured and wounded soldiers from the battlefield. Accurate knowledge of a soldier's health status enables medical rescue teams to perform rapid triage, which is critical in accident scenarios where swift and effective on-site medical assessment is essential. The study [1, 2] presented the proposed architecture of a system supporting medical evacuation, which utilizes continuous monitoring of key vital parameters. Among these parameters, alongside *heart rate* (HR), skin temperature, blood pressure (based on cuff-less method [3, 4]), and respiratory rate (based on strain sensor [5, 6] or *electrocardiographic* (ECG) signal [7, 8]), is arterial *blood oxygen saturation* (SpO₂).

The measurement of SpO₂ is a critical parameter in the context of medical evacuation [1], especially in military scenarios. A pulse oximeter, a relatively simple device, is used to measure this parameter along with heart rate [9-12]. The value of SpO₂ is given as a percentage, with a normal range considered to be between 94–100%. The pulse oximeter measures SpO₂ by detecting pulsatile blood flow in the capillaries, indicating that there is sufficient circulation and that the patient has not yet been struck down. This is crucial because shock is a state of systemic impairment of blood circulation, which needs to be identified early in trauma situations [13].

SpO₂ values reflect the efficiency of oxygen uptake in the lungs. Low SpO₂ levels can indicate respiratory failure, hypoxemia, or other issues that require immediate medical attention [14, 15]. In a combat situation, ensuring that a soldier's respiratory function is maintained is crucial for survival and for prioritising medical interventions. Early identification of hypoxemia allows for timely intervention, which is vital in combat zones where advanced medical care might not be readily available. Rapid and accurate SpO₂ measurements can influence the prioritisation of medical evacuation, ensuring that those in critical condition receive prompt care [16].

Moreover, triage systems used in civilian hospitals and emergency departments, such as the *Manchester Triage System* (MTS) [17], *Emergency Severity Index* (ESI), *Canadian Triage and Acuity Scale* (CTAS) [18], and *National Early Warning Score 2* (NEWS 2) [19, 20] incorporate SpO₂ measurement as a key indicator for assessing patient status. In military medical evacuation, similar triage protocols are *employed to classify* injured soldiers based on the urgency of their medical needs. Accurate SpO₂ measurement helps in the rapid classification of patients, ensuring that those with severe respiratory distress or other critical conditions are identified quickly and receive the necessary medical attention.

The precision of SpO₂ measurements can be affected by various factors such as low peripheral perfusion due to shock, hypothermia, carbon monoxide poisoning, cyanide poisoning, bright ambient light, massive blood loss, and movement of the pulse oximeter. These conditions are often encountered in combat zones, highlighting the need for robust and reliable pulse oximeters designed for military use. Despite potential challenges, SpO₂ measurement remains a non-invasive, quick, and essential method for assessing vital signs in the field. It provides immediate feedback on the circulatory and respiratory status of the soldier, facilitating timely and appropriate medical responses [21, 22].

In conclusion, SpO₂ measurement is vital in the context of military medical evacuation. It enables early detection of life-threatening conditions, supports effective triage, and ensures that soldiers receive the necessary care promptly. Given the challenging environments in which military operations occur, having reliable and accurate SpO₂ monitoring devices is indispensable for improving survival rates and outcomes during medical evacuations.

In pulse oximeters, in addition to the SpO₂ parameter, HR, or more precisely – *pulse rate* (PR) [14, 23] is also determined. This is because the calculation of SpO₂ requires the identification of individual pulses in the *photoplethysmography* (PPG) signal, which can also be used to calculate PR (as the number of individual PPG pulses in one minute). It is also worth noting, that determining individual pulses in the PPG signal allows the calculation of *pulse rate variability* (PRV) [24-26] as an alternative to *heart rate variability* (HRV) [27, 28]. The PRV calculation may be a useful feature in new pulse oximeters. Since this work mainly concerns the validation of the SpO₂ parameter, PR and PRV parameters were not determined.

The rest of this paper is organized as follows. In Section 2, the SpO₂ measurement principles are described. Section 3 describes the hardware design of the proposed sensor, signal processing method, test bench, validation study, and accuracy and statistical analysis. The experimental results and discussion are presented in Section 4. Finally, the conclusions of this study are presented in Section 5.

2. Background on SpO₂ measurement

The importance of SpO₂ measurement and its applications have been well-known and extensively described in the literature for decades [11, 12, 29]. SpO₂ measurement typically utilizes the PPG signal [30, 31], which represents blood flow in peripheral vessels and is obtained using optical techniques. The measurement of SpO₂ relies on determining the absorption of light at several wavelengths, which is selectively absorbed by *oxyhemoglobin*

(HbO₂) and *deoxyhemoglobin* (Hb). This absorption is determined based on the PPG signal, which can be related to the transmission of light through tissue or the reflection of light from internal tissue structures.

To measure the PPG signal, a sensor is used, consisting of a light source that illuminates the tissue and a photodetector that receives the transmitted or reflected light. Traditional PPG sensors (transmissive) are based on light transmission, where light passes through the tissue. They can be used in relatively thin areas with a high density of blood vessels, such as the finger or earlobe. Another type is reflective sensors, where the light source and photodetector are placed on the same side of the tissue. Reflective PPG sensors can be placed anywhere on the body with a high density of blood vessels, such as the forehead or in tactical watches.

Most SpO₂ measurements are performed in stable ambulatory or home conditions using a transmissive sensor placed on the fingertip. Measuring SpO₂ in dynamic conditions is much more challenging due to two main factors: (1) the type and location of the sensor, and (2) significant motion artifacts [32]. In dynamic conditions, such as during soldier combat operations, sensors worn by soldiers should not restrict their movement or cause discomfort. Therefore, SpO₂ measurements can only use reflective sensors placed in selected locations, such as the wrist [33] or forehead [34]. Due to the higher blood perfusion in the forehead compared to the wrist, the PPG signal, which is essential for pulse oximetry measurements, is significantly better on the forehead. The forehead appears to be a suitable location for placing the sensor because it has a relatively large surface area and is easily accessible, minimizing the risk of sensor displacement during movement.

An important aspect of SpO₂ measurement is perfusion, the blood flow through a particular part of the body [11, 12, 30]. The higher the perfusion index, the more accurate the SpO₂ measurement [35]. In the case of finger sensors, perfusion is driven by the radial artery and digital arteries. In contrast, forehead pulse oximeters utilize the supraorbital arteries. Forehead vessels have adequate perfusion, allowing for accurate SpO₂ measurement [36]. Additionally, the forehead is less prone to temperature changes and mechanical damage, which can positively affect the stability and accuracy of measurements.

Studies [37, 38] show that the PPG signals from sensors placed on the forehead and finger can provide different quality signals due to specific anatomical properties and blood perfusion in these areas. The sensor placed on the finger ensures higher perfusion and, thus, more accurate SpO₂ measurements than the forehead sensor. However, these more accurate measurements are obtained in static conditions. In dynamic conditions, such as during movement or physical activity, the finger sensor is susceptible to motion artifacts, reducing its measurement accuracy. Conversely, the forehead sensor provides better stability during movement, making it more suitable for use in dynamic conditions. Previous studies [39] on the accuracy of SpO₂ measurement depending on location show differences in values of up to 3.8±3.3%. Furthermore, the results presented in [39] indicate that forehead pulse oximeters may be more reliable compared to finger pulse oximeters during treadmill exercise tests. Also, it should be noted, that the blood vessels in the hand are more susceptible to unwanted pressure than in the forehead, which may result in incorrect SpO₂ readings [40].

In the context of military applications, a forehead sensor ensures discretion and ease of use. It can be easily integrated with helmets or other protective gear, allowing continuous monitoring of vital signs without hindering the performance of tasks. Additionally, by minimizing interference with hand movements, the forehead sensor enables soldiers to operate equipment freely without the risk of accidental displacement or damage to the device.

Forehead pulse oximeters are not yet widely popular. Among commercial solutions, the LNCS® TFA-1™ by *Masimo* [41] and MAXFAST by *Medtronic* [42] stand out. However, these are closed solutions and are not suitable for integration with other sensors, especially for wearable sensor/electronics applications. The study [43] presented a forehead pulse oximeter

designed for SpO₂ monitoring in newborns using the commercial fhPPG device (*SurePulse Medical Ltd*). There are also examples of custom projects, but they have their limitations. The study [34] presented a patch-type wireless wearable pulse oximeter system designed for forehead use. However, the proposed solution was tested on only six subjects, and SpO₂ levels were lowered by breath-holding. The study [44] presented a forehead pulse oximeter composed of three commercial integrated sensors (MAX30102) and analyzed SVM (*support vector machine*) and CNN (*convolutional neural network*) methods for assessing the quality of the measured PPG signals. Test studies conducted on 12 subjects showed that the SVM method is more effective than CNN.

Building on these findings, it is evident that further research and development are necessary to create robust, reliable SpO₂ solutions capable of delivering accurate vital-sign monitoring under challenging conditions, including military deployments.

3. Materials and methods

3.1. Hardware design of the SpO₂ sensor

Accurate SpO₂ measurement primarily depends on the quality of the PPG signals. The quality of the signal is influenced by many factors, including the biological characteristics of the tissue, measurement conditions, and the PPG sensor itself. Key components that determine the quality of the PPG signal are the LEDs emitting light onto the tissue and the photodetector receiving the reflected light. Green LEDs with wavelengths of 520–530 nm are commonly used for HR measurements. As shown in studies [45], PPG signals obtained with green light exhibit higher resistance to motion artifacts and thus yield more accurate HR measurements in both resting and dynamic conditions, which is why the green signal in this study serves as the basis for detecting individual PPG peaks. For SpO₂ measurement, the colours of the lights are determined by the measurement method. Red light with a wavelength of 600–750 nm and infrared light with a wavelength of 850–1000 nm are required [46]. It should be noted, that light at these wavelengths penetrates much deeper than green light, making the PPG signal obtained at these wavelengths highly susceptible to motion artifacts. Therefore, wearable devices with SpO₂ and HR measurement functions commonly use the three aforementioned colours of light. Additionally, in some cases, photodiodes with selective sensitivity characteristics are used for each light colour to eliminate components unrelated to the light of interest from the PPG signal.

Due to the high interest in SpO₂ and HR measurement in wearable devices such as smartwatches, dedicated modules integrating LEDs and photodiodes into a single small package have emerged in the electronic components market. For example, ams-OSRAM AG offers modules such as SFH 7050A, SFH7060A, SFH7072, and SFH7074.

In the presented solution, the SFH7072 module was used, containing two photodetectors with different sensitivity characteristics ($\lambda_{Smax} = 960$ nm - broadband photodiode, and $\lambda_{Smax} = 635$ nm - IR-cut photodiode) and four LEDs: two green (wavelength: 526 nm), one red (wavelength: 660 nm), and one infrared (wavelength: 950 nm).

The photodiodes in the SFH7072 module convert the optical PPG signal into an electrical signal. To calculate SpO₂, it is necessary to convert the electrical signal to digital using ADCs (*Analog-to-Digital Converter*). Often, the electrical signal from the sensor has low amplitude, so it must be amplified and filtered before digital conversion. Additionally, for SpO₂ measurement, it is necessary to obtain two PPG signals representing the same heart cycle: one for red light (660 nm) and the other for infrared light (950 nm). Sampling cannot occur simultaneously, as the lights would overlap, resulting in a combined PPG signal from both lights. Therefore, succeeding the generation of different coloured lights is necessary.

Furthermore, the electrical signal generated at the photodetector output must be multiplexed according to the currently generated light colour.

The amplifier circuit, filters, ADC, and sampling cycle control can be implemented as separate electronic components of the SpO₂ sensor. However, integrated circuits performing these functions are currently available on the market. These are referred to as *Analog Front-End* (AFE) systems. In this solution, the AFE4410 device from *Texas Instruments* was used. The overall connection diagram of the SpO₂ sensor components is shown in Fig. 1.

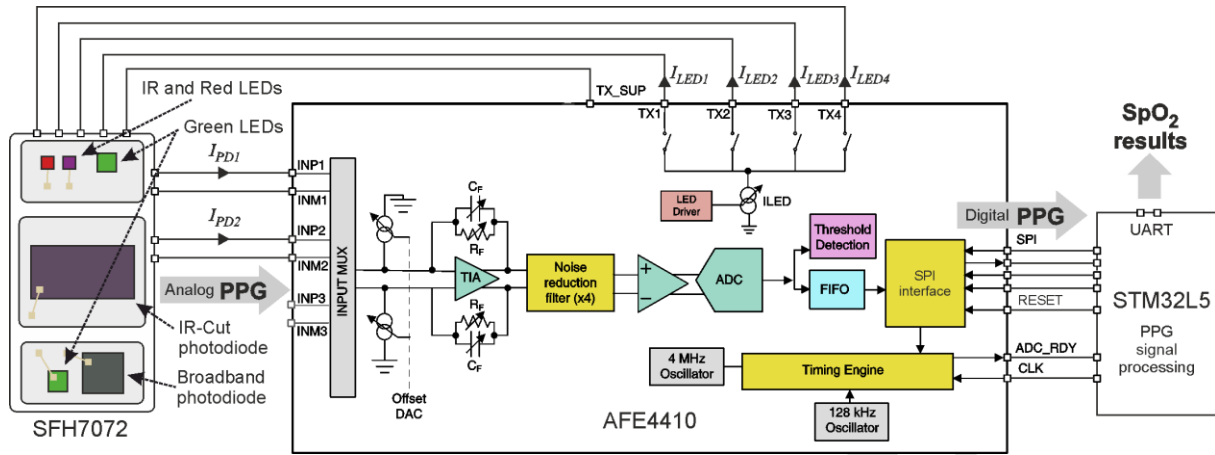


Fig. 1. SpO₂ sensor block diagram.

The electrical PPG signals from the photodiodes in the SFH7072 module are fed into a multiplexer, which directs them to the *transimpedance amplifier* (TIA) based on the currently illuminated LED. The TIA amplifies and converts the photodiode current to voltage. The amplifier gain can be adjusted using feedback resistors R_F . The *direct current* (DC) component of the PPG signal, representing the non-pulsatile part of the optical signal, can be removed (or added) before entering the amplifier using DACs (*Digital-to-Analog Converter*) connected to the TIA input. After amplification, the signal is sent to the ADC. Digital samples of the PPG signal are stored in a FIFO (*First In First Out*) buffer, from which they are retrieved by the STM32L5 microcontroller (STM32L552). The microcontroller is notified of sample storage in the FIFO buffer by a short change in the ADC_RDY line.

LED intensity is controlled by the LED driver. The timing controller successively lights the LEDs and initiates conversion processes, configured by a set of control registers of the AFE4410. Configuration register values can be read or changed via the SPI (*Serial Peripheral Interface*) interface.

The AFE4410 is configured to sample three PPG signals for each light colour separately (green, red, infrared) and an ambient light signal. The ambient light signal is the signal received by the photodetector when the LEDs are off. This measured signal is subtracted from the normal PPG signals, eliminating the influence of external ambient light on the SpO₂ measurement result. The current through the LEDs (I_{LED}) is set to 8 mA, while the current for DC component elimination (I_{OFFDAC}) is set to 1 μ A. The TIA gain is automatically adjusted based on the signal level at the TIA input. The photodiode current (I_{PD}) is calculated according to the formula:

$$I_{PD} = \frac{1.2V \times ADC_{val}}{2R_F(2^{21}-1)} + I_{OFFDAC}, \quad (1)$$

where ADC_{val} is the numerical value from the ADC output, R_F is the feedback resistor value of the TIA, and I_{OFFDAC} is the DC component elimination current value.

The presented SpO₂ sensor is designed as two separate *printed circuit boards* (PCBs). The larger one contains the microcontroller and the necessary circuits for power supply and

communication with the main device, while the smaller one includes the SFH7072 module and the AFE4410 chip. Both PCBs are shown in Fig. 2. They are connected by wires and mounted on an elastic band, which allows the sensor to be easily worn on the head.

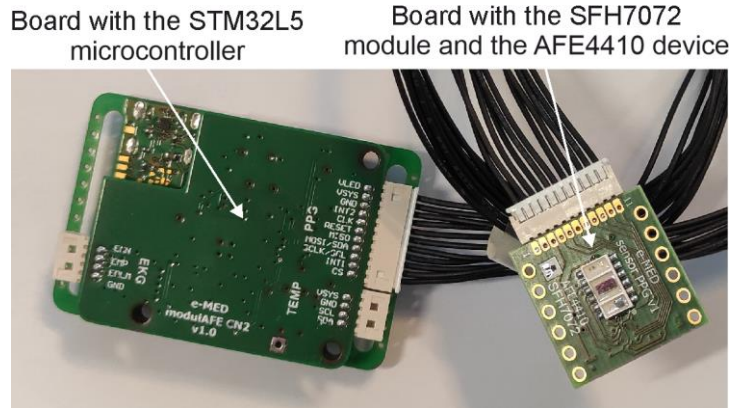


Fig. 2. Two PCBs of the SpO₂ sensor.

3.2. Signal processing method

SpO₂ measurement utilizes differences in light absorption by HbO₂ and Hb. HbO₂ absorbs more infrared light (950 nm) than Hb. Conversely, red light (660 nm) is more absorbed by Hb than HbO₂. Based on this relationship, it is possible to determine the R ratio, which is dependent on SpO₂. The R ratio is calculated using the formula:

$$R = \frac{AC_{red}/DC_{red}}{AC_{ir}/DC_{ir}}, \quad (2)$$

where AC_{red}, AC_{ir} denote the pulsatile components of the photoplethysmographic signal resulting from red and infrared light illumination, respectively, while DC_{red}, DC_{ir} represent the non-pulsatile components of the red and infrared PPG signals. Knowing the R value, SpO₂ can be determined from the empirical relationship between SpO₂ and R , described by the equation:

$$SpO_2 = a - b \times R, \quad (3)$$

where a and b are constants determined during calibration. For the initial device calibration, the WhaleTeq AECG100 simulator was used. Calibration resulted in $a = 116.96$ and $b = -33.07$.

Digital PPG signals obtained from the AFE4410 are processed by the microcontroller to determine SpO₂. The simplified digital signal processing diagram is shown in Fig. 3.

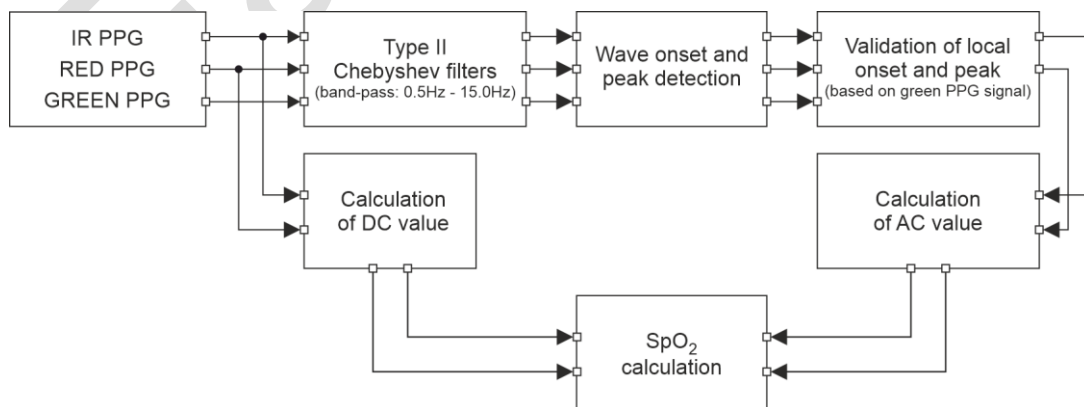


Fig. 3. Scheme of PPG signal processing.

In the first stage, the DC components of the RED and IR PPG signals (DC_{red} , DC_{ir}) are calculated. The signals are then subjected to band-pass filtering using a type II Chebyshev filter with a passband of 0.5 Hz to 15 Hz. Next, detection of the onset and peaks of the pulse wave is performed by analyzing the second derivative of the filtered signals in real time. By monitoring changes in this second derivative, points corresponding to the systolic peaks and wave onsets can be identified [47]. In addition, heart-rate constraints (e.g., 30–200 bpm) are applied to reduce false positives. These points are determined separately for each signal separately. For SpO_2 calculation, it is necessary to determine the onset and peaks of the PPG wave for the red and infrared signals. However, in the proposed solution, the points are also identified for the green PPG signal. The green signal points are used to validate the red and infrared PPG signal points. It is assumed that the green PPG signal is more resistant to motion artefacts, so its points will be more accurately determined. Based on the validated points, the AC components of the red and infrared PPG signals (AC_{red} , AC_{ir}) are calculated. In the final stage, the SpO_2 value is calculated according to formulas (2) and (3). The SpO_2 result is calculated for each PPG beat, i.e., for each heartbeat.

During preliminary studies, it was found that patient movement significantly affected SpO_2 measurement results, occasionally producing values far below 60% and above 100%. Therefore, it was decided that the algorithm would return a result of 60% for calculated values below 60% and 100% for values above 100%.

3.3. Measurement setup

The measurement setup consists of three main components, as shown in Fig. 4.

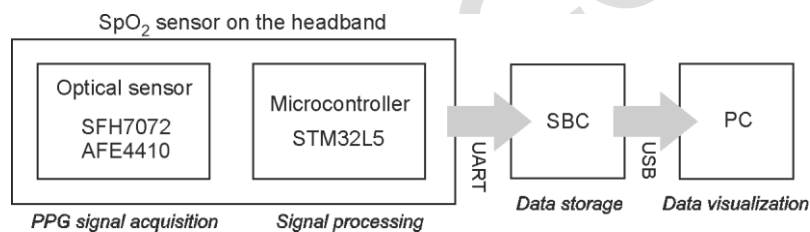


Fig. 4. Block diagram of the measurement setup.

The first component is the SpO_2 sensor mounted on a headband worn on the forehead. The second component is a custom-designed *Single Board Computer* (SBC), and the third is a PC (*Personal Computer*).

The SBC is responsible for reading PPG signal samples and SpO_2 values from the SpO_2 sensor. It records these signals onto a memory card and provides real-time data visualization on a PC via a USB interface. The connection to the headband is established using a UART serial interface. The SBC queries the SpO_2 sensor at a frequency of 100 Hz, receiving a set of PPG signal values and SpO_2 values in response. To ensure the safety of the subject, galvanic isolation of the power supply delivered through the USB interface has been implemented. Additionally, data lines are separated using optoelectronic isolators.

The third component of the measurement setup is a PC equipped with *SerialPlot* software. This software allows for the visualization of received data via the serial interface in the form of graphs. The ability to monitor PPG waveforms, SpO_2 values in real-time enables verification of the correct placement of the headband on the test subject.

Operating the measurement system involves a few simple steps: (1) placing the headband on the subject's head, (2) connecting the headband to the SBC, and (3) connecting the SBC to the PC to verify the accurate recording of PPG signals and the calculated SpO_2 parameter.

3.4. Validation study organization and subject characteristics

In the validation study, 18 healthy, active, and physically fit male subjects participated, each providing written informed consent. The average age (95% confidence interval - CI) was 37 (36-39) years, the average height (95% CI) was 181 (179-183) cm, and the average weight (95% CI) was 85 (83-87) kg. A total of 36 measurement cycles were conducted, yielding 215 valid data points.

To ensure the reliability and validity of the study, specific inclusion and exclusion criteria were established.

Exclusion Criteria:

- Symptoms of upper respiratory tract infection within the last two weeks.
- Smoking within the last 24 hours.
- Chronic diseases (e.g., hypertension, chronic respiratory diseases such as asthma and chronic obstructive pulmonary disease).
- Poor psycho-physical condition.
- Abnormal Allen's test (indicating insufficient circulation in the arterial arch of the hand).

Criteria for Termination of the Study:

- Completion of the designated 20-minute duration.
- Decision of the subject.
- Heart rate exceeding 120/min or dropping below 50/min.
- SpO₂ level falling below 80% for at least one minute or a drop in PaO₂ below 60 mmHg in arterial blood gas.
- General symptoms such as shortness of breath, headache, nausea, visual disturbances, chest pain, tinnitus, or dizziness.

None of the subjects met the exclusion criteria, and all measurements were completed within the designated 20-minute period. The study was conducted at sea level in Gdynia, Poland, at a room temperature of 21-23°C.

After explaining the study protocol, particularly the conditions for terminating the test, each subject underwent the Allen's test to ensure proper circulation. Following a negative result, under aseptic conditions and after local anesthesia, a physician performed radial artery cannulation in the non-dominant upper limb.

Subjects assumed a comfortable sitting position, with the validated SpO₂ sensor affixed to their forehead. All measurements were taken under stationary conditions, with subjects remaining at rest throughout the data collection. Additional medical monitoring equipment, specifically a patient monitor model LIFEPAK 15 Monitor/Defibrillator and Corpuls 3 Defibrillator, was used to measure the subjects' basic vital parameters including SpO₂. For comparison with the validated SpO₂ sensor, a reference device measuring oxygen saturation of arterial blood (SaO₂) was used, specifically ABL90 FLEXPLUS radiometer.

The sensors for the additional monitoring equipment were placed on the left finger and earlobe, and ECG electrodes were attached to the chest. Blood pressure was measured before and after the test. Subjects used a nose clip to close their nostrils and breathed through a scuba mouthpiece. They began breathing a prepared respiratory gas mixture from a tank. The test lasted for 20 minutes, with continuous SpO₂ measurement. SpO₂ values from both the validated SpO₂ sensor and the additional monitoring equipment were recorded every two minutes (for 30 seconds). Arterial blood gas analysis was performed every five minutes. At the moment arterial blood gasometry was taken, the SpO₂ measured by the test prototype was read. Measurements during the experiment were taken at rest. Measurements continued until a stable saturation level of 80% was achieved for one minute using prepared respiratory gas mixtures (TRIMIX 12%

oxygen, Nitrogen 46% and Helium 42%) or until 20 minutes of measurement were reached. The gas mixtures were prepared by a certified technician and analyzed prior to use to confirm the expected O₂ partial pressure.

3.5. Accuracy and statistical analysis

We evaluated the diagnostic accuracy of the validated pulse oximeter according to the standards specified in ISO 80601-2-61:2017, which replaces the ISO 80601-2-61:2011 standard recommended by the *U.S. Food and Drug Administration* (FDA) in the 510(k) Premarket Notification Submissions Guidance for pulse oximeter assessment [48]. This standard specifies that the A_{RMS} value should be used to evaluate the measurement accuracy of pulse oximeters. A_{RMS} is the root-mean-square difference between measured values y_p and reference value \bar{y}_p , as given by (4).

$$A_{RMS} = \sqrt{\frac{1}{n} \sum_{p=1}^n (y_p - \bar{y}_p)^2}, \quad (4)$$

where: A_{RMS} – root mean square difference, n – number of samples, y_p – pulse oximeter measurement, \bar{y}_p – reference standard measurement (saturation in arterial blood gasometry).

This standard considers an $A_{RMS} \leq 3.5\%$ acceptable for reflectance pulse oximeters (as in the studied example) within the SaO₂ range of 70%-100%. The measurement difference was defined as the difference between the reading of the prototype tested and the gold standard, which was the oxygen saturation of hemoglobin (SaO₂) in the collected arterial blood. Because A_{RMS} is highly susceptible to outlier results, an additional analysis was performed after excluding outliers defined as those whose difference between a pair of measurements exceeded ± 1.96 standard deviation (SD) from the group mean.

Statistica (version 13) and MS Excel (Office 365) programs were used to perform statistical analyses. For continuous variables with normal or non-normal distributions, mean values and 95% confidence intervals or median values and *interquartile ranges* (IQRs) were calculated, respectively. For nominal variables, counts and percentages were analyzed. Linear regression was used to evaluate trends. When assumptions of normality were not met, non-parametric tests (Chi-square, Mann-Whitney U, Spearman correlation) were used. A two-sided p -value of less than 0.05 was considered statistically significant.

4. Results and discussion

After performing validation tests, 215 pairs of results (validated SpO₂ sensor and reference measurements) were collected. The SD of the differences between the measurements obtained using the tested pulse oximeter and the arterial blood gas saturation values was calculated to be 4.1%. Initially, the A_{RMS} for all samples was calculated, which equaled 4.3%. Due to the high sensitivity of this parameter to outliers, those pairs of measurements whose difference exceeded the range of ± 1.96 SD were excluded. This resulted in 208 pairs of measurements for which the A_{RMS} equaled 3.0%. Based on these pairs, an analysis of the differences between the measured SpO₂ value and the reference value was performed using the Bland Altman plot [49]. The results obtained are shown in Fig. 5.

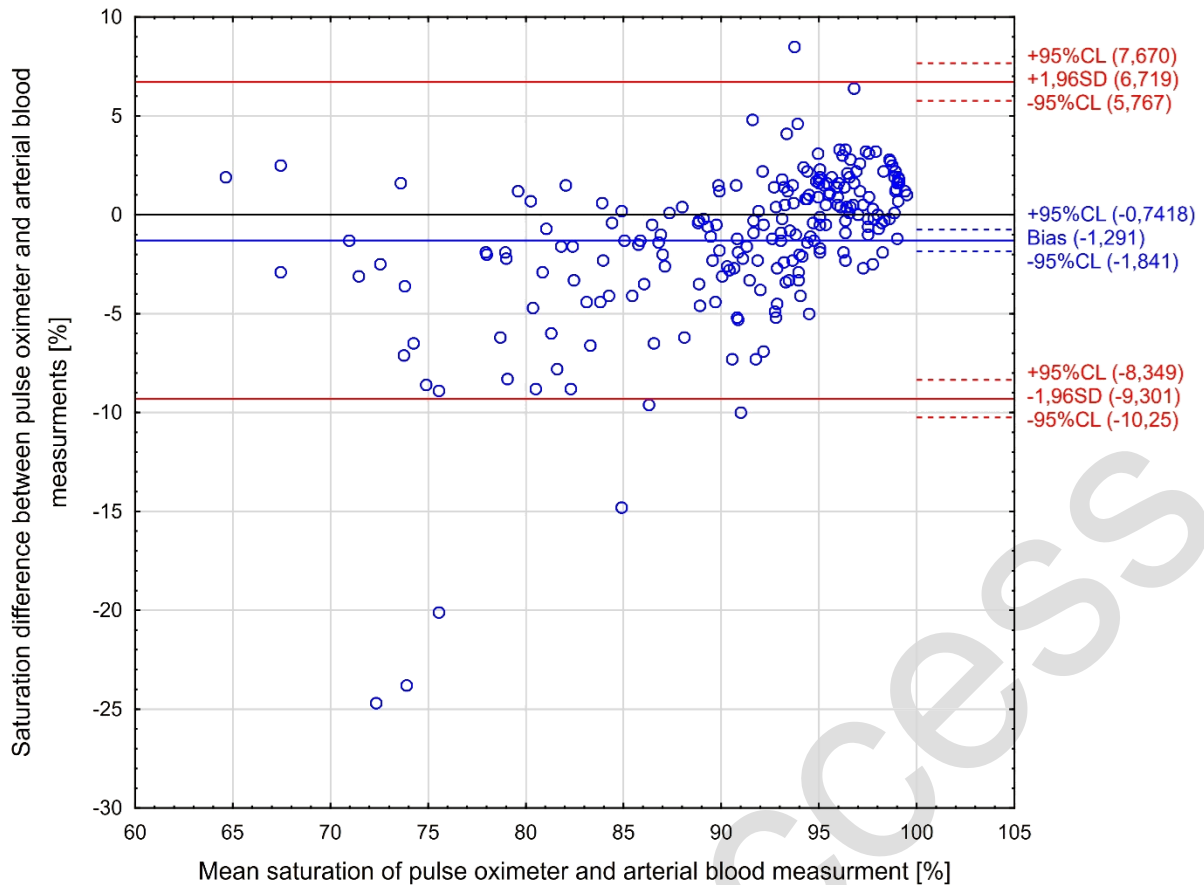


Fig. 5. Bland-Altman plot comparing measurements of pulse oximeter and arterial blood gasometry.

The criterion set by the FDA and ISO 80601-2-61 for reflectance pulse oximeters ($A_{RMS} \leq 3.5\%$ for measurements between the tested device and reference values) has been met.

Figure 6 shows the differences in measurement results for the tested device and the reference values at each measurement time point. The values did not differ significantly depending on the time point of measurement.

Our findings indicate that the validated SpO₂ sensor meets the required accuracy standards under stable conditions. However, during the tests, it was observed that patient movement significantly affected the measurement results, with accuracy deteriorating when the patient moved. Several studies, such as [50], have examined the performance of SpO₂ sensors under motion and low perfusion conditions and found that advanced algorithms significantly improved accuracy in these challenging environments. Our study did not incorporate such algorithms, focusing instead on the baseline performance of our sensor in stable conditions.

However, our study has limitations, including the specific demographic of the test subjects and the controlled environmental conditions. Future research should focus on testing the sensor in dynamic conditions to evaluate its performance under movement and varying perfusion states. This would provide a more comprehensive assessment of its applicability in real-world scenarios. Additionally, the next step will be to develop algorithms for eliminating motion artifacts, which should further improve the accuracy of SpO₂ measurements during patient movement.

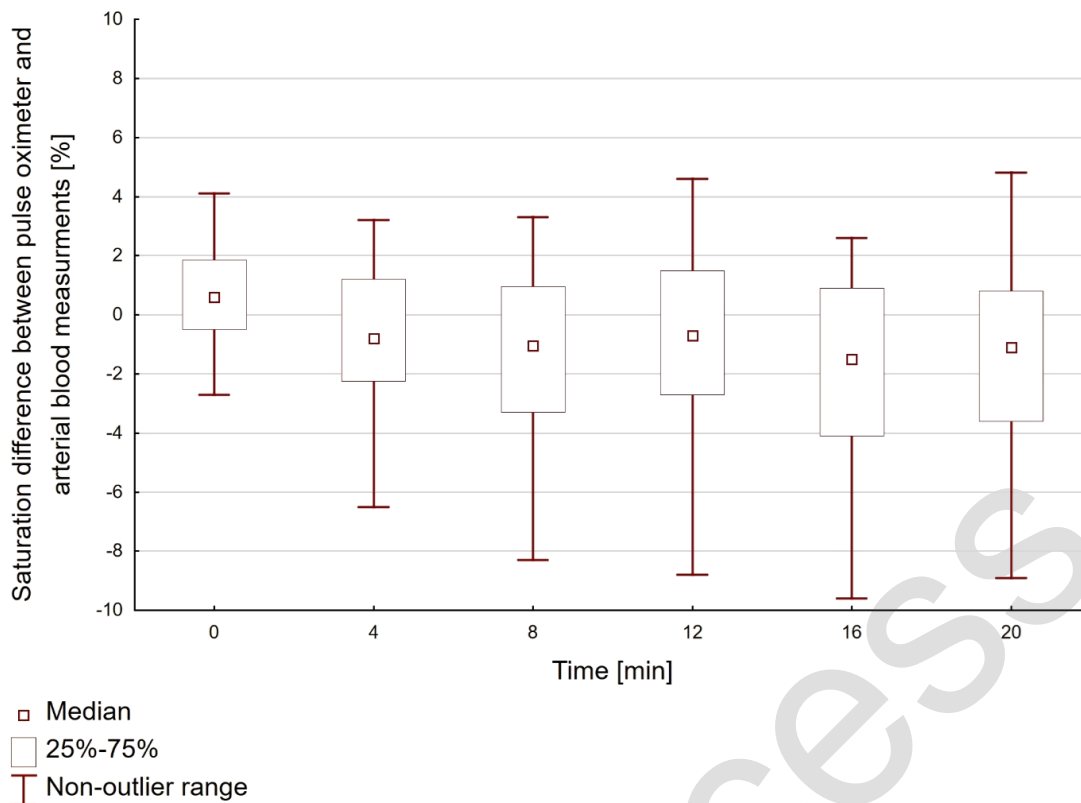


Fig. 6. Box plot of differences between pulse oximeter and arterial blood measurements at the following sampling points.

5. Conclusions

The conducted study demonstrated that the tested prototype of the reflectance pulse oximeter met the expected diagnostic criteria. The research showed that the device performs measurements in a stable manner, with the obtained parameters being consistent with those from validated commercial devices and corresponding to the reference values obtained through arterial blood gasometry. The statistical criterion specified in the guidelines and ISO 80601-2-61 was met, recommending an acceptable A_{RMS} result of $\leq 3.5\%$ for reflectance sensors. The tested prototype achieved an A_{RMS} value of 3.0%.

These findings indicate that the prototype can be successfully applied for clinical assessment of pulse oximetry values. However, since the tests were conducted under stationary conditions, practical application in field scenarios requires further research in a tactical environment. Future work will involve testing the sensor under dynamic conditions to evaluate its performance during movement and reduced perfusion, as well as the development of motion-artifact reduction algorithms to improve measurement accuracy during real-world use.

References

- [1] Lubkowski, P., Krygier, J., Sondej, T., Dobrowolski, A. P., Apiecioneck, L., Znanięcki, W., Oskwarek, P. (2023). Decision Support System Proposal for Medical Evacuations in Military Operations. *Sensors* (Basel, Switzerland), 23(11), 5144. <https://doi.org/10.3390/s23115144>
- [2] Krygier, J., Lubkowski, P., Maslanka, K., Dobrowolski, A. P., Mrozek, T., Znanięcki, W., & Oskwarek, P. (2024). Smart Medical Evacuation Support System for the Military. *Sensors* (Basel, Switzerland), 24(14), 4581. <https://doi.org/10.3390/s24144581>

- [3] Bard, D. M., Joseph, J. I., & van Helmond, N. (2019). Cuff-Less Methods for Blood Pressure Telemonitoring. *Frontiers in cardiovascular medicine*, 6, 40. <https://doi.org/10.3389/fcvm.2019.00040>
- [4] Yao, L. P., & Pan, Z. L. (2021). Cuff-less blood pressure estimation from photoplethysmography signal and electrocardiogram. *Physical and engineering sciences in medicine*, 44(2), 397–408. <https://doi.org/10.1007/s13246-021-00989-1>
- [5] Chu, M., Nguyen, T., Pandey, V., Zhou, Y., Pham, H. N., Bar-Yoseph, R., Radom-Aizik, S., Jain, R., Cooper, D. M., & Khine, M. (2019). Respiration rate and volume measurements using wearable strain sensors. *NPJ digital medicine*, 2, 8. <https://doi.org/10.1038/s41746-019-0083-3>
- [6] Hussain, T., Ullah, S., Fernández-García, R., & Gil, I. (2023). Wearable Sensors for Respiration Monitoring: A Review. *Sensors*, 23(17), 7518. <https://doi.org/10.3390/s23177518>
- [7] Szmajda, M., Chylinski, M., Sacha, J., & Mroczka, J. (2023). Three methods for determining the respiratory waves from ECG (Part I). *Metrology and Measurement Systems*, 30(4), 821–837. <https://doi.org/10.24425/mms.2023.147956>
- [8] Szmajda, M., Chylinski, M., Sacha, J., & Mroczka, J. (2024). Three methods for determining the respiratory waves from ECG (Part II). *Metrology and Measurement Systems*, 31(1), 51–71. <https://doi.org/10.24425/mms.2023.148544>
- [9] Chan, E. D., Chan, M. M., & Chan, M. M. (2013). Pulse oximetry: understanding its basic principles facilitates appreciation of its limitations. *Respiratory medicine*, 107(6), 789–799. <https://doi.org/10.1016/j.rmed.2013.02.004>
- [10] Nitzan, M., Romem, A., & Koppel, R. (2014). Pulse oximetry: fundamentals and technology update. *Medical devices (Auckland, N.Z.)*, 7, 231–239. <https://doi.org/10.2147/MDER.S47319>
- [11] Tekin, K., Karadogan, M., Gunaydin, S., & Kismet, K. (2023). Everything About Pulse Oximetry-Part 1: History, Principles, Advantages, Limitations, Inaccuracies, Cost Analysis, the Level of Knowledge About Pulse Oximeter Among Clinicians, and Pulse Oximetry Versus Tissue Oximetry. *Journal of Intensive Care Medicine*, 38(9), 775–784. <https://doi.org/10.1177/08850666231185752>
- [12] Tekin, K., Karadogan, M., Gunaydin, S., & Kismet, K. (2023). Everything About Pulse Oximetry-Part 2: Clinical Applications, Portable/Wearable Pulse Oximeters, Remote Patient Monitoring, and Recent Advances. *Journal Of Intensive Care Medicine*, 38(10), 887–896. <https://doi.org/10.1177/08850666231189175>
- [13] Indrawan, J., Solihat, Y., Wijaya, D.W., Nasution, A. H. & Sembiring, S. (2020). Pulse Oximetry Effectivity For Measuring Oxygen Saturation In Hypovolemic Shock Patient Compared To Blood Gas Analysis At Rsup H. Adam Malik Medan. *International Journal of Scientific and Research Publications*, 10(8). <http://dx.doi.org/10.29322/IJSRP.10.08.2020.p10499>
- [14] Tamura T. (2019). Current progress of photoplethysmography and SpO₂ for health monitoring. *Biomedical engineering letters*, 9(1), 21–36. <https://doi.org/10.1007/s13534-019-00097-w>
- [15] Allen J. (2007). Photoplethysmography and its application in clinical physiological measurement. *Physiological measurement*, 28(3), R1–R39. <https://doi.org/10.1088/0967-3334/28/3/R01>
- [16] Motta, L. P., Silva, P. P. F. D., Borguezan, B. M., Amaral, J. L. M. D., Milagres, L. G., Bóia, M. N., Ferraz, M. R., Mogami, R., Nunes, R. A., & Melo, P. L. (2021). An emergency system for monitoring pulse oximetry, peak expiratory flow, and body temperature of patients with COVID-19 at home: Development and preliminary application. *PloS one*, 16(3), e0247635. <https://doi.org/10.1371/journal.pone.0247635>
- [17] Mackway-Jones, K., Marsden, J., & Windle, J. (Eds.). (2013). *Emergency triage: Manchester triage group*. John Wiley & Sons. <https://doi.org/10.1002/9781118299029>
- [18] Gilboy, N., Tanabe, P., Travers, D., & Rosenau, A. M. (2011). *Emergency severity index (ESI): A triage tool for emergency department care, Version 4*. Implementation Handbook 2012 Edition. AHRQ Publication.
- [19] Royal College of Physicians (2017). *National Early Warning Score (NEWS) 2: Standardising the assessment of acute-illness severity in the NHS*. Updated report of a working party. London.
- [20] Smith, G. B., Prytherch, D. R., Meredith, P., Schmidt, P. E., & Featherstone, P. I. (2013). The ability of the National Early Warning Score (NEWS) to discriminate patients at risk of early cardiac arrest, unanticipated intensive care unit admission, and death. *Resuscitation*, 84(4), 465–470. <https://doi.org/10.1016/j.resuscitation.2012.12.016>

- [21] Jubran A. (2015). Pulse oximetry. *Critical care*, 19(1), 272. <https://doi.org/10.1186/s13054-015-0984-8>
- [22] Butler, F. K., Bennett, B., & Wedmore, C. I. (2017). Tactical Combat Casualty Care and Wilderness Medicine: Advancing Trauma Care in Austere Environments. *Emergency medicine clinics of North America*, 35(2), 391–407. <https://doi.org/10.1016/j.emc.2016.12.005>
- [23] Azudin, K., Gan, K. B., Jaafar, R., & Ja'afar, M. H. (2023). The Principles of Hearable Photoplethysmography Analysis and Applications in Physiological Monitoring-A Review. *Sensors*, 23(14), 6484. <https://doi.org/10.3390/s23146484>
- [24] Kumar, Ch., Mullagiri, M., Maruthy, K., Siva Kumar, A.V. & Kuppusamy, M. (2021). Association of Heart rate variability measured by RR interval from ECG and pulse to pulse interval from Photoplethysmography, *Clinical Epidemiology and Global Health*, 100698. <https://doi.org/10.1016/j.cegh.2021.100698>
- [25] Polak, A. G., Klich, B., Saganowski, S., Prucnal, M. A., & Kazienko, P. (2022). Processing Photoplethysmograms Recorded by Smartwatches to Improve the Quality of Derived Pulse Rate Variability. *Sensors*, 22(18), 7047. <https://doi.org/10.3390/s22187047>
- [26] Prucnal, M. A, Polak, A. G., & Kazienko, P. (2025), Improving the quality of pulse rate variability derived from wearable devices using adaptive, spectrum and nonlinear filtering, *Biomedical Signal Processing and Control*, vol. 102, 107336. <https://doi.org/10.1016/j.bspc.2024.107336>
- [27] Schoffl, J., Pozzato, I., Rodrigues, D., Arora, M., & Craig, A. (2023). Pulse rate variability: An alternative to heart rate variability in adults with spinal cord injury. *Psychophysiology*, 60(11), e14356. <https://doi.org/10.1111/psyp.14356>
- [28] Antali, F., Kulin, D., Lucz, K. I., Szabó, B., Szűcs, L., Kulin, S., & Miklós, Z. (2021). Multimodal Assessment of the Pulse Rate Variability Analysis Module of a Photoplethysmography-Based Telemedicine System. *Sensors*, 21(16), 5544. <https://doi.org/10.3390/s21165544>
- [29] Bachir, W. (2023). Diffuse transmittance visible spectroscopy using smartphone flashlight for photoplethysmography and vital signs measurements. *Spectrochimica acta. Part A, Molecular and biomolecular spectroscopy*, 303, 123181. <https://doi.org/10.1016/j.saa.2023.123181>
- [30] Allen J., & Kyriacou P. (2021). *Photoplethysmography: Technology, Signal Analysis and Applications*, Academic Press. <https://doi.org/10.1016/C2020-0-00098-8>
- [31] Kozioł, M., Piech, P., Maciejewski, M., & Surtel, W. (2019). The latest applications of photoplethysmography, *Acta Angiologica*, 25(1), 28-34. <https://doi.org/10.5603/AA.2019.0005>
- [32] Santos, M., Vollam, S., Pimentel, M. A., Areia, C., Young, L., Roman, C., Ede, J., Piper, P., King, E., Harford, M., Shah, A., Gustafson, O., Tarassenko, L., & Watkinson, P. (2022). The Use of Wearable Pulse Oximeters in the Prompt Detection of Hypoxemia and During Movement: Diagnostic Accuracy Study. *Journal Of Medical Internet Research*, 24(2), e28890. <https://doi.org/10.2196/28890>
- [33] Kałamajska, E., Misiurewicz, J., & Weremczuk, J. (2022). Wearable Pulse Oximeter for Swimming Pool Safety. *Sensors*, 22(10), 3823. <https://doi.org/10.3390/s22103823>
- [34] Azhari, A., Yoshimoto, S., Nezu, T., Iida, H., Ota, H., Noda, Y., ... & Morii, K. (2017, October). A patch-type wireless forehead pulse oximeter for SpO₂ measurement. In *2017 IEEE Biomedical Circuits and Systems Conference (BioCAS)* (pp. 1-4). IEEE. <https://doi.org/10.1109/BIOCAS.2017.8325557>
- [35] Hummler, H. D., Engelmann, A., Pohlandt, F., Högel, J., & Franz, A. R. (2006). Decreased accuracy of pulse oximetry measurements during low perfusion caused by sepsis: Is the perfusion index of any value?. *Intensive Care Medicine*, 32, 1428-1431. <https://doi.org/10.1007/s00134-006-0254-y>
- [36] Seifi, S., Khatony, A., Moradi, G., Abdi, A., & Najafi, F. (2018). Accuracy of pulse oximetry in detection of oxygen saturation in patients admitted to the intensive care unit of heart surgery: comparison of finger, toe, forehead and earlobe probes. *BMC Nursing*, 17, 1-7. <https://doi.org/10.1186/s12912-018-0283-1>
- [37] Longmore, S. K., Lui, G. Y., Naik, G., Breen, P. P., Jalaludin, B., & Gargiulo, G. D. (2019). A comparison of reflective photoplethysmography for detection of heart rate, blood oxygen saturation, and respiration rate at various anatomical locations. *Sensors*, 19(8), 1874. <https://doi.org/10.3390/s19081874>
- [38] Přibil, J., Přibilová, A., & Frollo, I. (2020). Comparative measurement of the PPG signal on different human body positions by sensors working in reflection and transmission modes. *Engineering Proceedings*, 2(1), 69. <https://doi.org/10.3390/ecsa-7-08204>

- [39] Kelly, K. L., Carlson, A. R., Allison, T. G., & Johnson, B. D. (2020). A comparison of finger and forehead pulse oximeters in heart failure patients during maximal exercise. *Heart & Lung*, 49(3), 259-264. <https://doi.org/10.1016/j.hrtlng.2019.10.012>
- [40] Sondej, T., & Zawadzka, S. (2021). Influence of cuff pressures of automatic sphygmomanometers on pulse oximetry measurements. *Measurement*, 187, 110329. <https://doi.org/10.1016/j.measurement.2021.110329>
- [41] Masimo (n.d.). *LNCS® TFA-1™ Disposable Forehead Sensor*. Retrieved June 18, 2024, from <https://techdocs.masimo.com/products/sensor/lncs-tfa-1-disposable-forehead-sensor/>
- [42] Medtronic (n.d.). *Nellcor™ Max-Fast™ forehead SpO₂ sensor*. Retrieved June 18, 2024, from <https://www.medtronic.com/covidien/en-us/products/pulse-oximetry/nellcor-spo2-forehead-sensor.html>
- [43] Stockwell, S. J., Kwok, T. C., Morgan, S. P., Sharkey, D., & Hayes-Gill, B. R. (2023). Forehead monitoring of heart rate in neonatal intensive care. *Frontiers in Physiology*, 14, 1127419. <https://doi.org/10.3389/fphys.2023.1127419>
- [44] Liu, S. H., Liu, H. C., Chen, W., & Tan, T. H. (2020). Evaluating quality of photoplethymographic signal on wearable forehead pulse oximeter with supervised classification approaches. *IEEE Access*, 8, 185121-185135. <https://doi.org/10.1109/ACCESS.2020.3029842>
- [45] Lee, J., Matsumura, K., Yamakoshi, K. I., Rolfe, P., Tanaka, S., & Yamakoshi, T. (2013, July). Comparison between red, green and blue light reflection photoplethysmography for heart rate monitoring during motion. In *2013 35th Annual International Conference of the IEEE Engineering in Medicine and Biology Society (EMBC)* (pp. 1724-1727). IEEE. <https://doi.org/10.1109/embc.2013.6609852>
- [46] Kirson, L. E., & Koltes-Edwards, R. (2010). *Pulse oximetry*. Anesthesia Secrets E-Book, 168.
- [47] Elgendi, M., Norton, I., Brearley, M., Abbott, D., & Schuurmans, D. (2013). Systolic peak detection in acceleration photoplethysmograms measured from emergency responders in tropical conditions. *PLOS One*, 8(10), e76585. <https://doi.org/10.1371/journal.pone.0076585>
- [48] U.S. Food and Drug Administration (2013, March). *Pulse Oximeters - Premarket Notification Submissions [510(k)s]: Guidance for Industry and Food and Drug Administration Staff*. <https://www.fda.gov/regulatory-information/search-fda-guidance-documents/pulse-oximeters-premarket-notification-submissions-510ks-guidance-industry-and-food-and-drug>
- [49] Ludbrook, J. (2010). Confidence in Altman–Bland plots: A critical review of the method of differences. *Clinical and Experimental Pharmacology and Physiology*, 37(2), 143-149. <https://doi.org/10.1111/j.1440-1681.2009.05288.x>
- [50] Louie, A., Feiner, J. R., Bickler, P. E., Rhodes, L., Bernstein, M., & Lucero, J. (2018). Four types of pulse oximeters accurately detect hypoxia during low perfusion and motion. *Anesthesiology*, 128(3), 520-530. <https://doi.org/10.1097/aln.0000000000002002>



Dominik Sondej received the M.Sc. and Ph.D. degrees in Electronic and Communication Engineering from the Military University of Technology (MUT), Warsaw, Poland, in 2012 and 2019, respectively. He is currently an Assistant Professor at the Faculty of Electronics of MUT, where he is involved in teaching, research, and supervision of diploma and doctoral theses. His scientific interests focus on

time and frequency metrology, time-to-digital and frequency-to-digital converters, embedded systems, as well as low-power biomedical signal processing. He has also contributed to research on cryptographic hardware security, including side-channel analysis. Dr. Sondej is a member of the Editorial Board of the international journal *Metrology and Measurement Systems* published by the Polish Academy of Sciences. He also serves as a reviewer for scientific journals and conferences in the fields of electronics and metrology.



Pawel Oskwarek – born in 1983 in Białka Podlaska, Poland. Since 2006, he has been based in Warsaw. He graduated from the Józef Piłsudski University of Physical Education, is a certified Paramedic, and holds a Master's degree in Nursing. He is also a Medical Simulation Instructor. He works at the Military Institute of Medicine – National Research Institute, in the Postgraduate Education Center, as

an Assistant in the Department of Battlefield Medicine and Medical Simulation.



Rafal Sokolowski, a doctor, graduated from the Military Medical Academy in 2000. In the years 2001-2011 - a doctor of the 1st Artillery Brigade. Since 2011 at Military Institute of Medicine in Warsaw. Currently the Head of The Pulmonology and Intensive Care Department at the Department of Pulmonology. He is interested in the treatment of respiratory failure, especially in the home aspect.



Michal Rząd obtained the medical degree and PhD in medical and health sciences from Medical University of Warsaw in 2019 and 2025, respectively. He is currently a doctor at the Department of Internal Medicine, Pneumology, Allergy, Clinical Immunology and Rare Diseases at the Military Institute of Medicine - National Research Institute in Warsaw. His research activities focus on pneumology, epidemiology, data

analysis and bioinformatics.



Adam Machowicz, M.D. is a graduate of the Faculty of Military Medicine at the Medical University of Łódź (formerly the Military Medical Academy). He is a specialist in anesthesiology and intensive care, with a professional background in both military and civilian healthcare. Until 2019, he served as a military physician and officer, holding key positions at the Military Medical Institute in Warsaw,

including Head of the Department of Battlefield Medicine and Medical Simulation. He contributed to the development of mobile surgical teams for the Armed Forces and participated in medical support for high-ranking state officials. Dr. Machowicz has lectured in postgraduate courses for medical personnel and has authored and co-authored several scientific publications and conference presentations. He currently works as an anesthesiologist and Deputy Medical Manager at one of Poland's leading plastic surgery hospitals.



Tadeusz Sondej received the M.Sc. degree in electronics and communications engineering, the Ph.D. degree and Habilitate Doctorate (D.Sc.) degree in applied science from the Military University of Technology (MUT), Warsaw, Poland, in 1997, 2013, and 2024 respectively. He is currently an university professor with the MUT. He has been involved in various research projects, mainly in the field of

measurement systems and autonomous electronic devices. His current research interests include the design and development of wearable electronics, autonomous digital systems, and methods and techniques for the measurement and processing of human physiological signals particularly for wearable healthcare devices.



Pawel Dabal received the M.S. and the Ph.D. degree in electronics and communication engineering from the Military University of Technology (MUT), Warsaw, Poland, in 2009 and 2018, respectively. His current research interests include microprocessor-based embedded systems, processing, and digital signal analysis in microprocessor systems.



Piotr Lubkowski received the Ph.D. degree from Military University of Technology, Warsaw, Poland, in 2002. He is professor in the Institute of Communications Systems, Faculty of Electronics, MUT. He is engaged in research in the area of multimedia systems and services as well as QoS in heterogeneous mobile wireless ad hoc networks. His current research activity is focused on effective transfer of

biomedical data over low bandwidth networks.